Journal of Materials Chemistry C

Accepted Manuscript

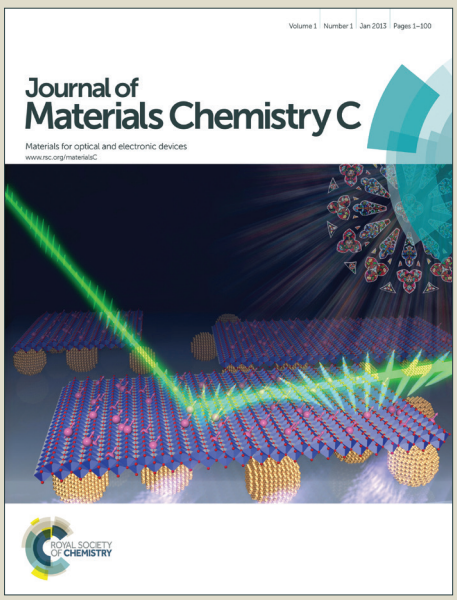

ROYAL SOCIETY OF CHEMISTRY

www.rsc.org/materialsC

ARTICLE Journal Name

Transparent nanocellulose hybrid films functionalized with ZnO nanostructures for UV-blocking

Cite this: DOI: 10.1039/x0xx00000x

Received 00th January 2012,
Accepted 00th January 2012

DOI: 10.1039/x0xx00000x

www.rsc.org/

Yaoquan Jiang,[a] Yuanyuan Song,[b] Miao Miao,[a] Shaomei Cao,[a] Xin Feng,[a,b,]* Jianhui Fang[c] and Liyi Shi[a]

Transparent nanocellulose-ZnO (NC/ZnO) hybrid films were fabricated via a pressure controlled extrusion process by using NC fibrils and sheet-like ZnO (s-ZnO) and belt-like ZnO (b-ZnO) nanostructures. The s-ZnO and b-ZnO conjoined with NC fibrils together to form a heterogeneous fibrous network structure, respectively. The NC/ZnO hybrid films with different amount of ZnO nanostructures showed a synergic feature of high optical transparency and excellent UV-blocking. The results indicated that NC assembled with s-ZnO hybrid film possessed an excellent UV-blocking property in the wide range from 200 to 375 nm in contrast with NC/b-ZnO. Moreover, the prominent thermal and photo stability of transparent NC/ZnO hybrid films enhanced extensibility and easy to use for diverse biological applications to tolerate temperature changes.

Introduction

With the decreasing of stratospheric ozone content in the atmosphere, more ultraviolet (UV) radiation from solar spectrum is the most striking and ubiquitous detrimental effects on human health and other biological systems.[1-4] Excessive exposure to sunlight increases strong biological damage and degradation of organic compounds by UVA (320~400nm) and UVB (280~320nm) radiation.[5-7] Therefore, the development of new generation self-protective sunscreen products such as visually transparent UV filters or coatings for UV-sensitive materials and lenses is still challenging. Because the petroleum based polymer matrix usually cannot endure high temperature,[8] a woven fabric essentially made from cotton or sisal fibers has become the primary means of protection in daily life. Unfortunately, the UV radiation can easily transmit through the ordinary woven fabrics.[9] Wang et al. prepared dumpbell-shaped ZnO with the aid of ZnO nanorods on the surface of cotton fabrics, the dumbbell-shaped ZnO presented a wider UV-blocking range (400-280 nm) than that of ZnO nanosols (352-280 nm), nanorods (375-280 nm), and anatase titania films (332-280 nm).[10] Mao et al. covered cotton fabrics with needle-shaped ZnO nanorods, the nano ZnO coated cotton fabrics have UV transmission in UVB region (315-250 nm) and part of UVA region (370-315 nm).[11] Recently, Li et al. developed an effective route to fabricated hierarchical flower-like ZnO on cotton cellulose fibers by combining electrospinning and the low-temperature growth technique. The results indicated that cotton cellulose coated with flower-like ZnO has high absorption at the wavelength of 350 nm.[12] Wang et al. coated cotton textile with ZnO@SiO_2 nanorods and found that the UV transmittance obviously decreased. They believed the excellent UV-blocking of the modified cotton textile ascribed to the good absorption and strong scattering of ZnO@SiO_2nanorods array.[13] Due to its high strength, large surface area and unique optical properties, nanocellulose (NC) extracted from diverse native sources, including cotton, wood, bamboo, sisal, algae and bacteria, has received considerable attention in the last few decades.[14-15]NC based films with firm and uniform network have excellent optical transparency for its nanometric fiber diameters, the light scattering is so decreased that large part of the light transmits with no scattering. Furthermore, the transparent NC films with low coefficients of thermal expansion (12-28.5 ppmK^{-1}) make it easy to process in high temperature than plastic substrates.[16] The functionalized NC based films is of great interest combined with the exciting synergetic characteristics including high transparency, outstanding biodegradability and excellent UV-blocking, which can be widely used for vast application possibilities such as outdoor UV-sensitive polymers, car windshields, clean windows, contact lenses, and some special biological test containers.[17] As a typical II-VI semiconductor, ZnO exhibits a large exaction-binding energy (60 meV) and wide band gap (3.37 eV).[18,19] It has attracted tremendous interests owing to its remarkable environmentally friendly nature and chemically stable under exposure to both high temperature and UV.[20,21] ZnO nanostructures with large surface area to volume ratio have an increasing UV-blocking effectiveness compared with that of bulk ZnO. [20]

All the work mentioned above has been demonstrated that woven fabrics combined with different ZnO nanostructures is beneficial to preventing UV radiation exposure. Till now, great efforts have been devoted to the development of synthetic methodologies for ZnO nanostructures due to their promising applications.[22-26] NC is an ideal building block to host a range of guest ZnO nanomaterials to create UV protective transparent films for coating UV-sensitive substrates. However, the major issue that need to be addressed for the assembly of NC hybrid films with heterogeneous network architectures still remain. The difficulty is the extremely slow dewatering because of the high water binding capacity of NC,[27] the conventional methods such as suspension-casting, water evaporation, and hot pressing to remove the excessive water is extremely time-consuming, which require from several hours to a few days and even longer with complicated manipulations.[28]

Herein, highly transparent NC-ZnO hybrid films for UV blocking were rapidly assembled via a pressured extrusion dewatering method under ambient temperature using readily available starting materials. Different ZnO nanostructures were combined with NC skeleton network to form heterogeneous fibrous hybrid films exhibiting synergic effect of ZnO and NC. The as-prepared hybrid films were characterized by XRD, FE-SEM, TG and UV-vis spectroscopy. By changing the amount of

ZnO in the transparent NC based matrices, the UV-blocking property was preliminary evaluated.

Experimental

Materials

All the reagents were of analytical grade and used without any further purification. Zinc acetate dihydrate, anhydrous ethanol, Urea, Sodium hydroxide, hydrogen peroxide, Sodium silicate, Trisodium phosphate, Triton X-100, Acetic acid, Polyvinyl Pyrrolidone, Nitric acid and Glycerol were purchased from Sinopharm Chemical Reagent Co, Ltd. (Shanghai, China), Sodium Chlorite was obtained from Aladdin Industrial Inc. (Shanghai, China).

Preparation of nanocellulose (NC)

Bamboo fibers were mechanical smashed to pass through 200-mesh screen, followed by washing with distilled water. 160 g dried bamboo fibers, 2000 g distilled water and 60 g NaOH were first added to three-necked round-bottomed flask to heat at 100 ºC for 2 h, filtered and washed with distilled water to neutral pH. Secondly, the base treated bamboo fibers were heated in 2000 mL distilled water, 1 wt% NaOH, 0.4 wt% Na_3PO_4 and 0.4 wt% (8 g) Na_2SiO_3 solutions (2000 mL) at 115 ºC for 2 h, filtered and washed with distilled water to neutral pH. Thirdly, the delignified fibers were treated with 3.5 wt% NaOH, 0.7 wt% $NaClO_2$ and 150 mL CH_3COOH aqueous solutions (2000 mL) at 100 ºC for 2 h, 0.5 wt% Triton X-100 and 5 wt% Citric acid aqueous solutions (2000 mL) at 70 ºC for 4 h, respectively, followed by washing with distilled water. After that, the bleaching was enhanced by continuing the reaction in 30 wt% H_2O_2 and 65 wt% HNO_3 aqueous solutions (2:1 v:v) at 70 ºC for 1 h, filtered and washed thoroughly to neutral pH. The chemical treated aggregates were defibrillated according to a homogenization process with high pressure homogenizer (D−3L, PhD Technology LLC, USA) for 3 cycles at a pressure of 5000 ppi to obtain NC suspensions.

Preparation of sheet-like ZnO (s-ZnO)

Sheet-like ZnO was synthesized according to a modified literature method.[29] 2.16 g $Zn(OAc)_2$•$2H_2O$ mixed with 1.90 g urea were dissolved in 50 mL H_2O and transferred to Teflon autoclave, a 5×5 cm^2 cotton fabric was immersed into the solution. After the autoclave was heated at 140 ºC for 24 h, the as-prepared precursor collected from cotton fabric was calcined at 350 ºC for 5 h to obtain s-ZnO.

Preparation of belt-like ZnO (b-ZnO)

Belt-like ZnO was prepared via a modified literature procedure,[30] 3.63 g $Zn(OAc)_2$•$2H_2O$, 6.43 g NaOH, 1.05 g PVP, 40 mL H_2O_2 and 400 mL distilled water were introduced to Teflon autoclave and heated at 140 ºC for 12 h. The sediment was washed with distilled water twice and dried at 70 ºC to obtain ZnO_2. After that, ZnO_2 was added to hydrazine hydrate (85%) with vigorous stirring, and then the resultant solution was transferred to Teflon autoclave and heated at 150 ºC for 24 h. Finally, b-ZnO was collected after washing and drying at 70 ºC for 4 h.

Fast assembly of NC/ZnO hybrid films

NC/ZnO hybrid films were rapidly assembled as illustrated by using an extrusion method.[31,32] 1.03 g NC suspension (2.93 wt%) was first diluted in 100 mL H_2O. And then 100 mL diluted NC solution, a certain quantity of s-ZnO or b-ZnO and 0.50 g glycerol were mixed and sonicated with a high frequency ultrasonic cell disruptor (High Nova instrument Co., Ltd, China) at 700 W for 5 min in order to make a homogeneous solution. The as-prepared uniform dispersion was poured into the extruder (NanoAble-150, PhD Technology LLC, USA) to squeeze out the excess water under 2.0 MPa of N_2 gas. Subsequently, a gel cake emerged on the filter membrane (PC, nuclepore track-etch membrane, pore size 200 nm, Whatman, UK) was peeled off and sandwiched between two glass plates thoroughly dried at 95 °C for 10 min in a vacuum oven (0.1 MPa). NC/ZnO hybrid films doping with different amount of ZnO labeled as NC/s-ZnOx and NC/b-ZnOx (x=0, 1, 2, 3, 4, 5, 6 wt%), respectively. The transparent hybrid films with 30 μm in thickness and 45 mm in diameter were ultimately prepared.

Characterization

The morphologies of the NC were observed with transmission electron microscopy (TEM) (JEM-200CX, JEOL, Japan) at an accelerating voltage of 120 kV. The morphologies of s-ZnO, b-ZnO and hybrid films were carried out by using a field emission scanning electron microscopy (FE-SEM) (JSM-6700F, JEOL, Japan). The phase structures of hybrid films were characterized by using a powder X-ray diffraction (XRD), which was carried out on a D/MAX2200 X-ray diffractometer equipped with Cu Kα1 (λ = 1.5418 Å) radiation operating at 40 kV and 40 mA. The diffuse Reflectance UV-visible spectra were obtained by using a UV-vis (2501PC, SHIMADZU, Japan) diode array spectrophotometer for dry pressed disk samples, which were prepared by mixing ZnO and $BaSO_4$ and its scans range was 200~800 nm. The UV-blocking properties of the hybrid films were investigated by measuring their absorbance and transmittance with a UV-vis (2501PC, SHIMADZU, Japan) spectrophotometer. A thermo nicolet 6700 spectrometer (Thermo Fisher Scientific, USA) was used to record FT-IR in transmission mode, ranging from 4000 to 400 cm^{-1}, using the pressed KBr tablets prepared by making finely grinded samples mixed with dry KBr powder. The thermal stability of the hybrid films was studied using NETZSCH STA409PC (Simultaneous Thermal Analyzer) instrument. The samples were measured at a heating rate of 10 ºC /min in the range of 30~700 ºC under air and N_2 atmosphere, respectively.

Results and discussion

Figure 1 shows TEM images of the NC obtained before and after homogenization process. As shown in Figure 1a and 1b, the as-prepared NC has uniform diameter distribution and conjoins together to form a network structure. The dimension of NC ranges from 30 to 50 nm in width and 1-6 μm in length before homogenization process. The homogenization impact could break the relatively weak interfaces between the fibers bonded mainly by Van der Waals forces, resulting in decentralizing of the overall NC fibers. It can be observed from Figure 1b that the diameter of NC after homogenizing becomes 10-30 nm, meanwhile the length decreases to 1-2 μm, which can be further in favor of the formation of transparent NC films.[33,34] SEM micrographs of s-ZnO and b-ZnO nanostructures are shown in Figure 2, respectively. It is obvious that s-ZnO consists mainly of closely-packed monolayer with 60 nm or so in thickness, and the synthetic b-ZnO has uniform distributed nanobelts. The lengths of the nanobelts are typically tens of micrometers, the average width is 300 nm and the average thickness is about 100 nm.

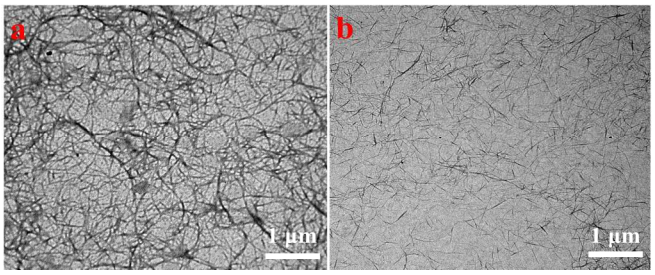

Figure 1. TEM images of NC (a) before and (b) after homogenization.

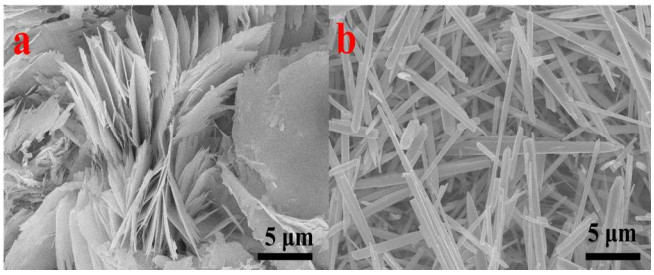

Figure 2. SEM images of (a) s-ZnO and (b) b-ZnO nanostructures.

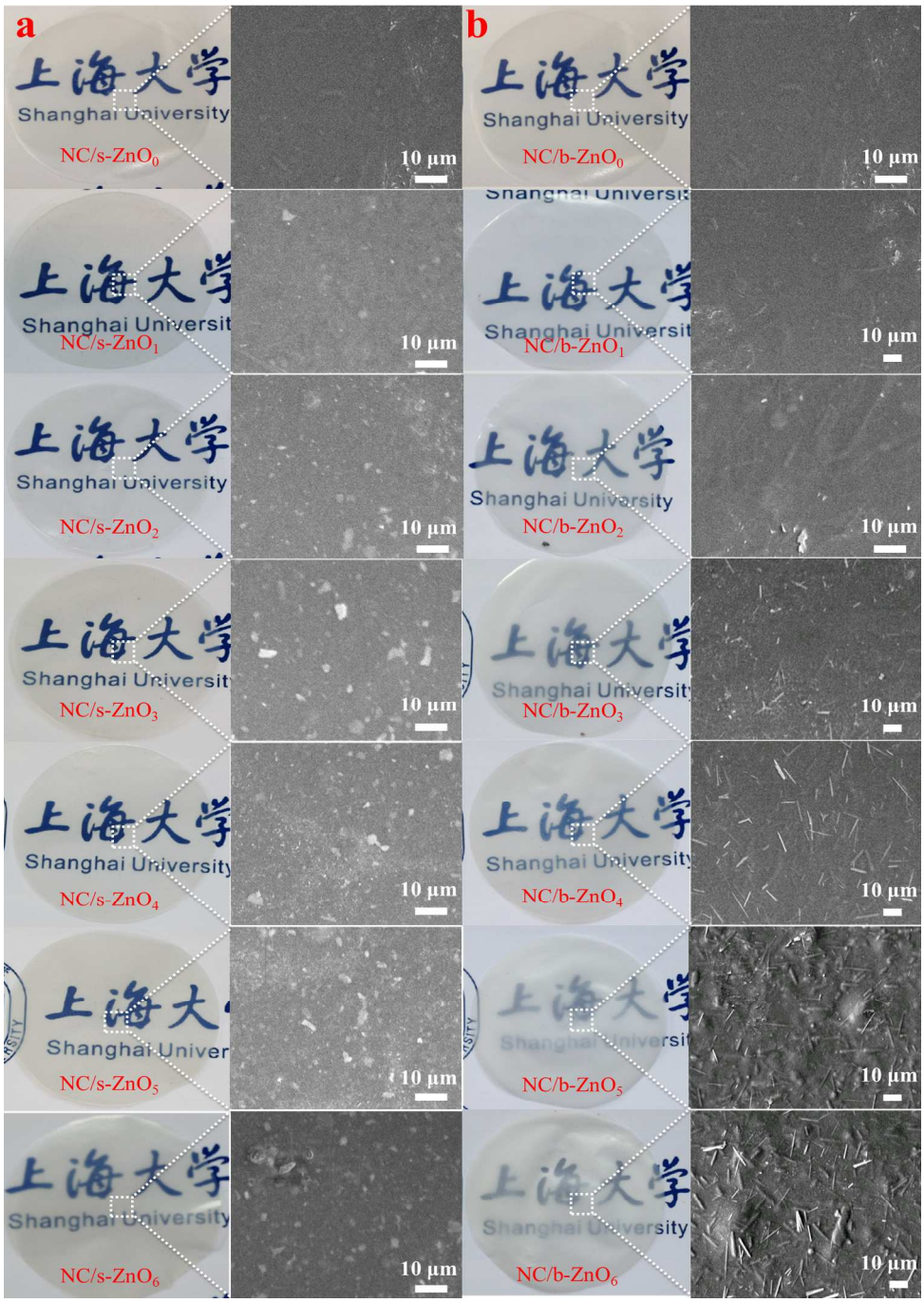

Figure 3. Digital pictures and the relative SEM images of NC/ ZnOx hybrid films with different s-ZnO (a) and b-ZnO (b) amount of 0, 1, 2, 3, 4, 5, 6 wt%, respectively.

Digital pictures of NC/ZnO hybrid films and the relative SEM images of the surface morphologies of the hybrid films are presented in Figure 3. It can be clearly showed that the NC films without the addition of ZnO nanostructures display highly optical transparency, indicating that the films consist of cellulose fibers with diameter in nanometric. The optical transparency of hybrid films was maintained by adding proper amount of ZnO nanostructures, indicating that ZnO combined uniformly with NC was beneficial to the decrease of light scattering of NC/ZnO hybrid films. However, the transmittance of the hybrid films was deceased with the increasing of stoichiometric ratio of ZnO immobilized into NC fibrous network, the results were verified from that the school emblem of Shanghai University under the hybrid films becoming more obscure. NC/b-ZnOx (x=0, 1, 2, 3, 4, 5, 6 wt%) hybrid films exhibit the most distinct characteristics and tendency compared to NC/s-ZnOx (x=0, 1, 2, 3, 4, 5, 6 wt%) as shown in the left column of Figure 3a and 3b. The right column of Figure 3a and 3b illustrate the surface morphologies of NC/s-ZnOx hybrid films and NC/b-ZnOx hybrid films, respectively. It can be observed that the surfaces of the NC films are quite smooth, but the flatness decreases with the addition of ZnO nanostructures. The whiter sheet-like (Figure 3a) or fibrillar (Figure 3b) materials are ZnO nanostructures which well dispersed and embedded on the hybrid films network without aggregation. NC fibrous network acts as a template allowing the high dispersity of ZnO nanostructures in the aqueous dispersion, so that the individual ZnO could adsorb stably on the NC fibrils by entangling with each other. It can be concluded that the high degree of transparency of hybrid films was ascribed to the high dispersity of ZnO nanostructures on the NC fibrous network. After increasing the additive amount of ZnO from 1 wt% to 6 wt%, a lot of ZnO nanostructures were gradually exposed on the surface of the hybrid films. It can also be seen from SEM image that plenty of protruding spots, which are NC fibrils, were uniformly dispersed on the cross-section of pure NC film (Figure S1a). Moreover, the cross-sectional SEM images of hybrid films (Figure S1b,c) represented well-stacked structure without aggregation of ZnO nanostructure. And the trace of s-ZnO drawn from the cross-section and the presence of b-ZnO embedded on the cross-section were obviously discerned. Consequently, the resulting microstructures and uniform distribution of ZnO nanostructures might be beneficial to the remarkable UV-blocking of the hybrid films.

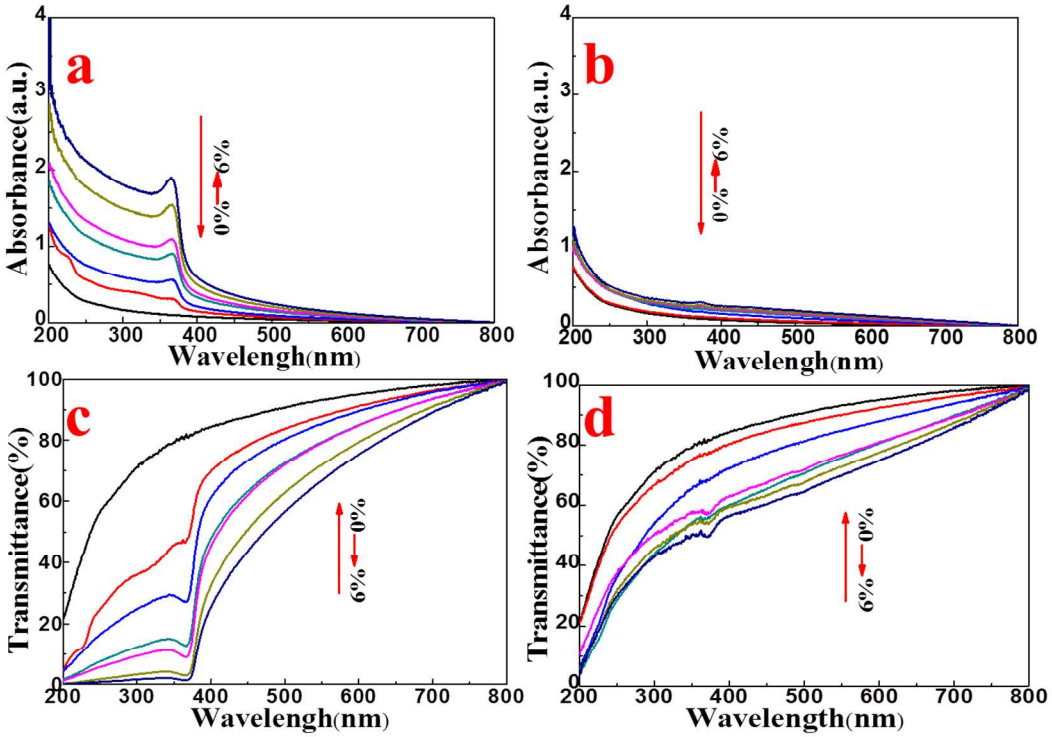

Figure 4. UV-vis spectra of NC/s-ZnOx (a,c) and NC/b-ZnOx (b,d) hybrid films with different amounts of ZnO (x=0, 1, 2, 3, 4, 5, 6 wt%).

UV spectra were recorded for the NC/ZnO hybrid films with different addition of ZnO nanostructures by measuring the transmission.[35] The absorbance of NC/ZnOx (x=0, 1, 2, 3, 4, 5, 6 wt%) hybrid films can be seen in Figure 4a and 4b, showing the ability of UV-blocking directly. It is obvious that a sharp absorption peak and a weak absorption peak with the increasing amount of s-ZnO and b-ZnO, respectively. The UV absorption band of NC/s-ZnO hybrid films almost covers the whole UV range up to 400 nm. Meanwhile, Figure 4c and 4d show the optical transmittance plotted against the wavelength for the NC/ZnOx (x=0, 1, 2, 3, 4, 5, 6 wt%) hybrid films with different ZnO nanostructures. It can be clearly seen that NC/s-ZnO hybrid films have excellent UV-blocking performance superior than that of NC/b-ZnO hybrid films. However, as ZnO nanostructures contents increase, the transmittance decreases dramatically. The neat NC films have high optical transparency and certain UV blocking ability. But by incorporating ZnO nanostructures into NC matrices, UV photons with wavelengths in the wide range from 200 to 375 nm are efficiently absorbed by NC/s-ZnO hybrid films. And high amount of s-ZnO results in enhanced UV-blocking efficiency, especially 90% of UV region. The results indicated that s-ZnO had better size and dimension effects compared to b-ZnO, thereby enhancing the UV-blocking efficiency.[36] The nanocomposites possessing high visible light transparency and high UV light resistance simultaneously are desirable for a range of important

applications.[26,36,37] The transmittance, Visible-shielding Ratio (VR) and UV-blocking Ratio (UVR) of NC/ZnO hybrid films are shown in Table 1. Here, *T*(%)-s550 and *T*(%)-b550 mean the transmittance of NC/s-ZnO and NC/b-ZnO hybrid films at 550 nm, respectively. UVR-s300 and UVR-b300 are UVR of NC/s-ZnO and NC/b-ZnO hybrid films at 300 nm, respectively. UVR-s225 and UVR-b225 are UVR of NC/s-ZnO and NC/b-ZnO hybrid films at 225 nm, respectively. The transmittance of NC/s-ZnO hybrid films is similar to those of NC/b-ZnO hybrid films at 550 nm. An equation (1) was used to evaluate the VR and UVR at 300 nm, 225 nm and 550 nm of the films:[9]

$$R(\%) = (T_0\text{-}T)/T_0 \quad (1)$$

Where T_0 is the transmittance as-prepared pure NC films, T is transmittance of (x=0, 1, 2, 3, 4, 5, 6 wt%) films. The UVR increase with the increasing additions of ZnO nanostructures, indicating that the UVR of NC/s-ZnO hybrid films at 300 nm and 225 nm are higher than those of NC/b-ZnO hybrid films, reached to 97.79% and 99.13%, respectively. The solid diffuse reflection UV-vis spectra (Figure S2) were further verified that s-ZnO possessed a better UV reflection compared to the b-ZnO, which corresponded to the evidence of NC/s-ZnO hybrid films had a higher UVR. The VR of NC/s-ZnO and NC/b-ZnO hybrid films at 550 nm were also evaluated. The results indicated that the VR increased with ZnO contents. Consequently, NC/s-ZnO hybrid films with s-ZnO contents of 3 wt% and 4 wt% exhibit high UV light absorption and low absorption of visible light, hence high UV-blocking efficiency and high visible light transparency. In addition, the optical properties of NC/s-ZnO hybrid films were investigated by bending for 200 times at the angle of 135°. It can be seen that the changes of transmittance and absorbance are negligible (Figure S3). Therefore, it can be reasonably foreseen that the UV-blocking property of the as-obtained transparent NC/s-ZnO hybrid films will pave the way for a large variety of applications in human health and other biological systems.

Table 1. The transmittance, Visible-shielding Ratio (VR) and UV-blocking Ratio (UVR) of NC/s-ZnO and NC/b-ZnO hybrid films.

	NC/ZnO_0	NC/ZnO_1	NC/ZnO_2	NC/ZnO_3	NC/ZnO_4	NC/ZnO_5	NC/ZnO_6
T(%)-s550	93.39	87.84	85.44	79.49	79.12	71.81	66.70
T(%)-b550	93.39	90.08	84.84	75.78	76.74	72.71	69.81
VR-s550	0	5.94	8.51	14.88	15.28	23.19	28.58
VR-b550	0	3.54	9.70	18.86	17.83	22.14	25.25
UVR-s300	0	49.28	65.17	82.56	86.87	95.37	97.79
UVR-b300	0	6.05	24.10	38.33	28.87	35.58	39.72
UVR-s225	0	70.98	74.88	89.56	91.82	97.98	99.13
UVR-b225	0	5.32	51.03	62.95	38.55	55.97	56.23

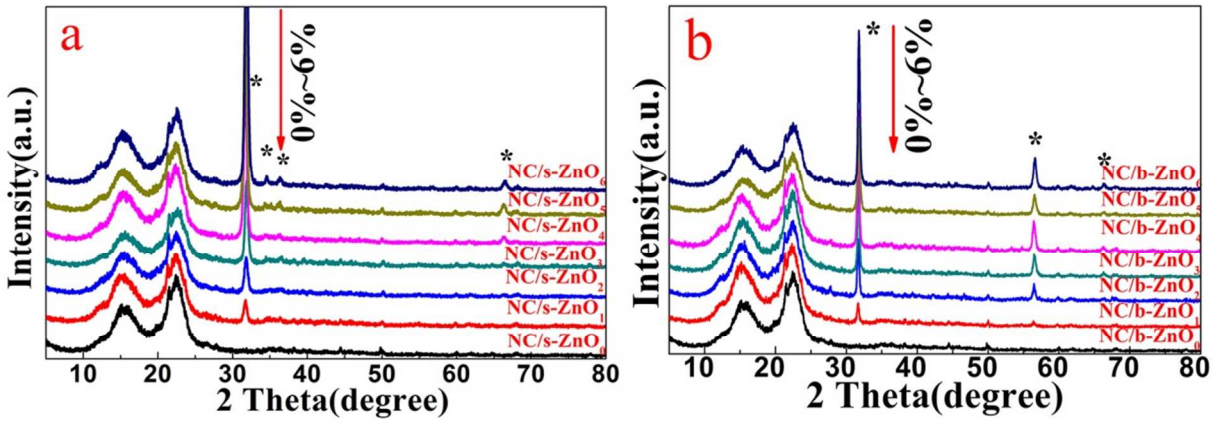

Figure 5. XRD patterns of NC/s-ZnOx (a) and NC/b-ZnOx (b) hybrid films with different amounts of ZnO nanostructures (x=0, 1, 2, 3, 4, 5, 6 wt%).

Figure 5 shows XRD patterns of NC/s-ZnOx and NC/d-ZnOx hybrid films, respectively. The peaks at 14.7º, 16.5º, 22.7º and 35.0º can be indexed the typical (101), (101), (200), and (040) reflections of cellulose I.[9,38] When increasing the addition of s-ZnO, the intensities of ZnO characteristic peaks at 31.8º, 34.4º, 36.4º and 66.2º gradually increase.[39] However, for NC/b-ZnOx hybrid films, there is a relative stronger peaks at 56.6º with the addition of b-ZnO (Figure 5b), compared with the main peaks of NC/s-ZnOx hybrid films as shown in Figure 5a. Therefore, it can be deduced that the b-ZnO nanostructures have different crystalline structure and a very highly c-axis growth-orientation. The results indicated that NC fibrils were successfully assembled with different ZnO nanostructures to form heterogeneous hybrid films.

The thermal stability of NC/ZnO hybrid films was an important factor for a diverse application to tolerate temperature changes. Figure 6 clearly demonstrates the thermal degradation of the NC/ZnO hybrid films under air and N_2 atmosphere with different amount of ZnO nanostructures. For comparative purposes, the TG curve of $NC/s\text{-}ZnO_0$ film under a N_2 atmosphere was also presented, which well corresponded to the reported literature.[40] The total weight loss of the NC film is 100 wt% after heating up to about 575 ºC, and 35wt% weight loss at about 300 ºC attributed to the desorption of moisture. All the samples exhibited a significant weight loss at about 320 ºC is ascribed to the decomposition of NC.[41] With the addition of ZnOx (x=1, 3%), the TG curves of hybrid films under a N_2 atmosphere are almost similar to that of NC film, but the thermal stability of NC/ZnO hybrid films increases. Under air atmosphere, another mass loss stage ranged from 350 °C to 470 °C could be observed. The second mass loss for the degradation of NC fibrils under oxidative atmosphere is

commonly designated to the oxidation of char formed by primary pyrolysis reaction.[42] The weight under N_2 and air atmosphere still remains about 1wt% and 3wt% at the temperature about 700 ºC, respectively. This evidence further indicated that ZnO nanostructures were successfully embedded into the NC fibrils to form a heterogeneous network structure.

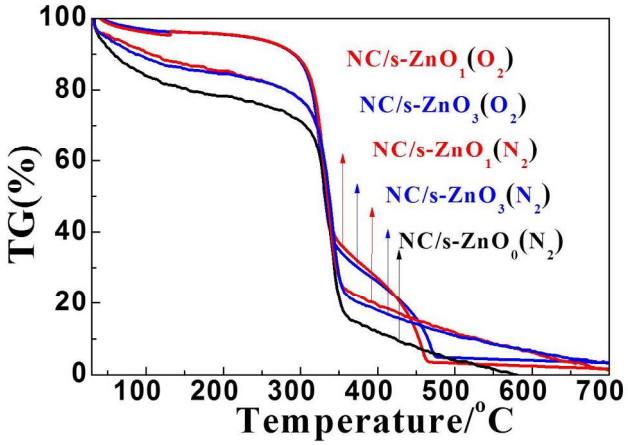

Figure 6. TG curves of NC/s-ZnO hybrid films with different ZnO nanostructures of 0 wt%, 1 wt%, and 3 wt%, respectively.

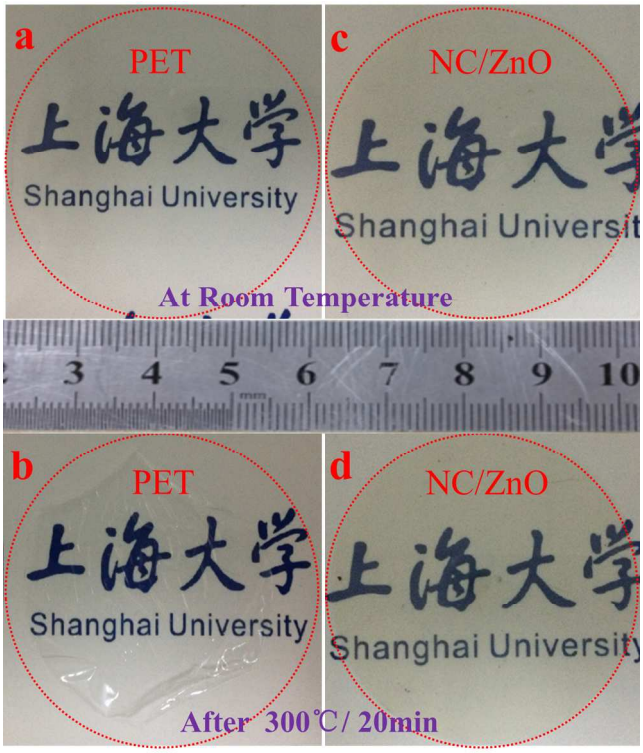

Figure 7. Digital pictures of PET film (a, b) and NC/s-ZnO (c, d) film at room temperature and after heating at 300 ºC for 20 min, respectively.

Figure 7 compares the thermal stability of NC/s-ZnO hybrid film with that of the PET film by measuring the dimensional change after heating at 300 ºC for 20 min. the PET film shows the large thermal shrinkage and wrinkle (Figure 7b), however, the dimensional change of the NC/ZnO hybrid film could be ignored (Figure 7d). The outstanding thermal stability of NC/s-ZnO hybrid films was due to the anomalous characteristics of NC.[43] Another interesting observation from this study is that NC/ZnO hybrid films have perfect photo stability under UV irradiation for about 72 h (Table S1). This is due to the superior UV light screening effects offered by the addition of ZnO nanostructures.

Conclusions

In summary, transparent NC/ZnO hybrid films were successfully fabricated via a pressure-controlled extrusion process using NC fibrils as soft matrix and s-ZnO or b-ZnO nanostructures as functional fillers. The different ZnO nanostructures were uniformly dispersed in the NC network structure measured by SEM. As a result, NC/s-ZnO hybrid films exhibited more prominent UV-blocking properties than NC/b-ZnO hybrid films with the same amount of ZnO. The as-prepared NC/s-ZnO hybrid films with s-ZnO contents of 3 wt% and 4 wt% possessed simultaneously high transparency and excellent UV-blocking property. The UV-blocking ratio of NC/s-ZnO hybrid films with s-ZnO content of 6 wt% was 97.79% and 99.13% at 300 nm and 225 nm, respectively, much higher than that of NC/b-ZnO hybrid films. Therefore, we demonstrate herein a facile strategy to prepare transparent NC/ZnO hybrid films, which could be applied for the realization of transparent, low-cost, lightweight, and flexible substrates in UV-blocking fields.

Acknowledgements

This work was financially supported by Shanghai Foundation of Excellent Young University Teacher and the Science and Technology Commission of Shanghai Municipality (13ZR1415100, 13JC1402700, 15ZR1415100, 13DZ2292100). The authors are also grateful to Instrumental Analysis & Research Center of Shanghai University.

Notes and references

[a]Research Center of Nano Science and Technology, Shanghai University, Shanghai 200444, P. R. China. Tel.: +86 21 66137257, Fax: +86 21 66136038, Corresponding Author:* E-mail: fengxin@shu.edu.cn

[b]School of Materials Sciences and Engineering, Shanghai University, Shanghai 200444, P. R. China.

[c]Department of Chemistry, Shanghai University, Shanghai 200444, P. R. China.

Electronic Supplementary Information (ESI) available: [SEM images of the cross-section of hybrid films, solid diffuse reflection UV-vis spectra, UV-vis spectra and photo-degradation results]. See DOI: 10.1039/b000000x/

1 J. B. Kerr1 and C. T. McElroy. *Science*, 1993, **262**, 1032.

2 M. Berneburg, H. Plettenberg, J. Krutmann, et al., *Photodermatol. Photoimmunol. Photomed.*, 2000, **16**, 239.

3 M. R. Albert, and K. G. Ostheimer, *J. Am. Acad. Dermatol.*, 2002, **47**, 930.
4 C. E. Williamson, P. J. Neale, G. Grad, et al., *Ecol. Appl.*, 2001, **11**, 1843.
5 F. R. de Gruijl, *Eur. J. Cancer*, 1999, **35**, 2003.
6 H. Stege, L. Roza, A. A. Vink, et al., *Proc. Natl. Acad. Sci.,* 2000, **97**, 1790.
7 H. Hattori, Y. Ide, T. Sano, et al., *J. Mater. Chem. A*, 2014, **2**, 16381.
8 K. Q. Han and M. H. Yu, *J. Appl. Polym. Sci.*, 2006, **100**, 1588.
9 Y. Li, Y. L. Zou, Y. Y. Hou, et al., *Cellulose*, 2011, **18**, 1643.
10 R. H. Wang, J. H. Xin, X. M. Tao, et al., *Inorg. Chem.,* 2005, **44**, 3926.
11 Z. P. Mao, Q. P. Shi, L. P. Zhang, et al., *Thin Solid Films*, 2009, **517**, 2681.
12 C. R. Li, Y. Xie, Q. Y. Liu, et al., *Fiber. Polym.,* 2014, **15**, 281.
13 L. L. Wang, X. T Zhang, B. Li, et al., *ACS Appl. Mater. Interfaces* 2011, **3**, 1277.
14 Y. Habibi, L. A. Lucia, O. J. Rojas et al., *Chem Rev.*, 2010, **110**, 3479.
15 Q. Song, W. T. Winter, B. M. Bujanovic, et al., *Energies,* 2014, **7**, 607.
16 J. Huang, H. G. Zhu, Y. C. Chen, et al., *ACS Nano*, 2013, **7**, 2106.
17 T. Y. Wang, T. T. Isimjan, J. F. Chen, et al., *Nanotechnology*, 2011, **22**, 265708
18 X. Feng, J. P, Zhang, W. Shi, et al., *Mater. Technol.*, 2010, **25**, 35.
19 X. Feng, L. Y. Shi, S. F. Wang, et al., *Solid State Ionics*. 2008, **179**, 2077.
20 A. Becheri, M. Dϋrr, P. L. Nostro, et al., *J. Nanopart. Res.*, 2008, **10**, 679.
21 Y. Tu, L. Zhou, Y. Z. Jin, et al., *J. Mater. Chem*., 2010, **20**, 1594.
22 Ü. Ö. Ya. I. Alivov, A. Liu, et al, *J. Appl. Physics*., 2005, **98**, 041301.
23 Z. J. Xing, B. Y. Geng, X. L. Li, et al., *Cryst. Eng. Commun.*, 2011, **13**, 2137.
24 Y. B. He, G. R. Li, Z. L. Wang, et al., *Energ. Environ. Sci.,* 2011, **4**, 1288.
25 C. M. Chang, M. H. Hon, I. C. Leu, et al., *Sens. Actuators B*., 2010, **151**, 15.
26 Z. X. Wang, X. Y. Zhan, Y. J. Wang, et al., *Nanoscale*, 2012, **4**, 2678.
27 M. Österberg, J. Vartiainen, J. Lucenius, et al., *ACS Appl. Mater. Interfaces*, 2013, **5**, 4640.
28 M. Nogi, S. Iwamoto, A. N. Nakagaito, et al., *Adv. Mater*., 2009, **21**, 1595.
29 J. H. Pan, X. W. Zhang, J. D Alan., et al., *Phys. Chem. Chem. Phys*., 2012, **14**, 7481.
30 X. Cao, N. Wang, L. Wang, et al., *J. Nanopart. Res.*, 2010, **12**, 143.
31 J. P. Zhao, Z. W. Wei, X. Feng, et al., *ACS Appl. Mater. Interfaces,* 2014, **6**, 14945.
32 M. Miao, J. P. Zhao, X. Feng, et al., *J. Mater. Chem. C*, 2015, **3**, 2511.
33 H. L. Zhu, S. Parvinian, C. Preston, et al., *Nanoscale*, 2013, **5**, 3787.
34 H. Koga, T. Saito, T. Kitaoka, et al., *Biomacromolecules*, 2013, **14**, 1160.
35 G. Y. Zhang. Y. Liu. H. Morikawa, et al., *Cellulose*, 2013, **20**, 1877.
36 Y. Q. Li, S.Y. Fu, Y.W. Mai, *Polymer*, 2006, **47**, 2127.
37 Y. Ren, M. Chen, Y. Zhang, et al., *Langmuir,* 2010, **26**, 11391.
38 Q. L. Lu, W. Y. Lin, L. R. Tang, et al., *J. Mater. Sci.*, 2015, **50**, 611.
39 A. Kumar, H. Gullapalli, K. Balakrishnan, et al., *Small*. 2011, **7**, 2173.
40 G. G. Alves, P. A. A. P. Marques, C. P. Neto, et al., *Crys. Growth Des.*, 2009, **9**, 386.
41 C. Katepetch, R. Rujiravanit, H. Tamura, et al., *Cellulose*, 2013, **20**, 1275.
42 D. K. Shen, J. M. Ye, R. Xiao, et al., *Carbohydr. Polym*., 2013, **98**, 514.
43 S.-J. Chun, E.-S. Choi, E.-H. Lee, et al., *J. Mater. Chem*., 2012, **22**, 16618.

Table of Contents

Transparent nanocellulose films functionalized with sheet-like ZnO nanostructures presented excellent UV-blocking performance in a wide range from 200 to 375 nm.